A Transient 3-D CFD Model for the Simulation of Forced or Natural Convection of the EU DEMO In-Vessel Components

Nicolò Garelli, Antonio Froio, Gandolfo Alessandro Spagnuolo, Roberto Zanino, *Senior Member, IEEE*, and Andrea Zappatore

***Abstract*— As the EU DEMO reactor will act as a Component Test Facility for the breeding blanket (BB), it is foreseen that the different BB concepts will be tested throughout the plant's lifetime. The maintenance of all the in-vessel components (IVCs), as for all D-T fusion machines, must be carried out employing remote handling (RH) technology, as the structural materials will be activated by the neutrons. The maintained segment and possibly other nearby segments cannot be actively cooled and will heat up due to the decay heat. For these reasons, alternative cooling strategies need thus to be investigated to ensure that the BB segment will cool down within the limits required by the RH in a reasonable amount of time. In the present work, two possible cooling options are investigated for the case of the Water-Cooled Lithium-Lead BB concept. One is based on the passive cool-down by natural convection of the BB segments, whereas the second one relies on a forcing flow of cool air on the BB surfaces. A computational fluid dynamics (CFD) approach has been used to study the different options for performing transient analyses through the Star-CCM+ commercial code.**

***Index Terms*— Computational fluid dynamics (CFD), EU DEMO, in-vessel components (IVCs), remote handling (RH).**

I. Introduction

THE EU DEMO is planned to be the first European fusion device to include a fully-functional breeding blanket (BB) by the 2050s [1], and as such it will act as a Component Test Facility for the BB [2], with BB replacement already foreseen throughout the plant lifetime. Due to the high radioactive dose that will be reached within the tokamak building, the replacement of the BB will be carried out through remote handling (RH). As the design of the RH systems is ongoing, an upper limit for the contact operating temperature between the RH tool and the BB segment is set to 150 °C [3].

As the RH will attach to the BB through the upper port on the segment chimneys [4] (see Fig. 1), where the cooling system pipes are also routed [5], the maintained BB segments need to be isolated from the primary heat transfer system (PHTS) and cannot be actively cooled; conversely, the other BB segments are assumed to be actively kept at about 300 °C (this conservative assumption maximizes the temperature of the adjacent BB segments and, therefore, the effectiveness of the two possible cooling strategies discussed in this article). Moreover, due to previous irradiation, some decay heat will be generated within the BB. Therefore, before the RH can operate [the remote maintenance (RM) operation is assumed to start after one month from the shutdown], the BB segments need to be cooled down, and this can be achieved with two possible strategies: 1) natural circulation and 2) forced circulation.

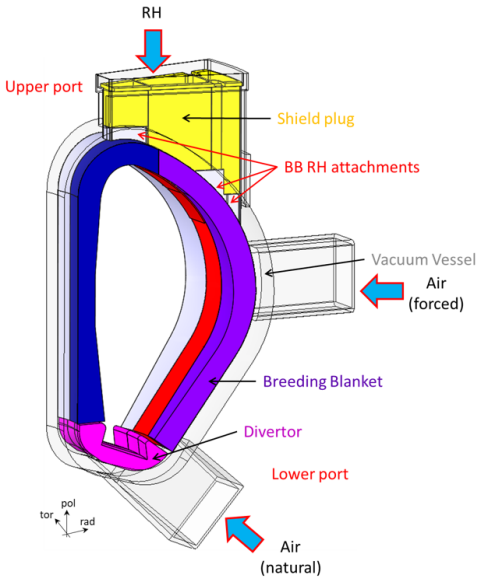

Fig. 1. Isometric view of an EU DEMO sector, with the vacuum vessel, its internals, the air inlets, and the BB RH attachments.

Manuscript received 27 January 2022; revised 19 July 2022; accepted 17 October 2022. Date of publication 1 November 2022; date of current version 30 November 2022. This work has been carried out within the framework of the EUROfusion Consortium, funded by the European Union via the Euratom Research and Training Programme (Grant Agreement No 101052200 – EUROfusion). Views and opinions expressed are however those of the author(s) only and do not necessarily reflect those of the European Union or the European Commission. Neither the European Union nor the European Commission can be held responsible for them. The work of Andrea Zappatore was supported by the EUROfusion Researcher Grant. The review of this article was arranged by Senior Editor G. H. Neilson. *(Corresponding author: Antonio Froio.)*

Nicolò Garelli was with the NEMO Group, Dipartimento Energia, Politecnico di Torino, 10129 Turin, Italy. He is now with newcleo, 10129 Turin, Italy (e-mail: nicolo.garelli@newcleo.com).

Antonio Froio, Roberto Zanino, and Andrea Zappatore are with the NEMO Group, Dipartimento Energia, Politecnico di Torino, 10129 Turin, Italy (e-mail: antonio.froio@polito.it; roberto.zanino@polito.it; andrea.zappatore@polito.it).

Gandolfo Alessandro Spagnuolo is with the PPPT Department, EUROfusion Consortium, 85748 Garching bei München, Germany (e-mail: alessandro.spagnuolo@euro-fusion.org).

Color versions of one or more figures in this article are available at https://doi.org/10.1109/TPS.2022.3215924.

Digital Object Identifier 10.1109/TPS.2022.3215924

In the first case, the air is let to enter the vacuum vessel (VV) through the upper and lower ports (assuming that the RM of the divertor is synchronized with the one of the BB) and the flow is driven by the temperature difference between the BB and the air itself (as well as by the decay heat); in the latter case, the flow of air in the VV is forced by an external machine.

In the present work, these two options are investigated for the case of the water-cooled lithium-lead (WCLL) BB concept [6], via a transient 3-D computational fluid dynamics (CFD) model developed with the commercial Star-CCM+ code [7]; previous works have investigated similar scenarios, that is, for the helium-cooled pebble bed (HCPB) BB concept [8], or for both concepts in [9]. In [9], however, different boundary conditions (BCs) were assumed (e.g., the temperature of nonmaintained segments, domain definition), and a different geometrical model was adopted, modeling also the cask environment and neglecting the plasma chamber volume beyond the sector under maintenance, while in the present work we take into account also the presence of the plasma chamber volume.

II. 3-D CFD Models

In view of the different setups required for the cases of natural and forced convection, two different models have been made, both solving the mass, momentum, and energy conservation equations (i.e., the set of incompressible Navier–Stokes equations). For the case of natural convection, the model is based on that developed for the HCPB BB concept, which is reported in [8], to which the reader is referred for further details. The only differences are the material properties and the decay heat, which are the same as for the forced convection model, which is described below. Therefore, only the forced convection model is described in this section, with emphasis on the differences with respect to the natural convection model.

The initial conditions are the same for the two cases and they are due to the steady state reached one month after the plasma shutdown: it is assumed that the cooling of all the components is kept active for one month, thus reaching 300 °C and ambient pressure in the plasma chamber, while the cooling of the divertor and the VV are kept at 26 °C and 40 °C, respectively. One month of active cooling of the components before starting RM on the BB is indeed needed as several other operations are required before the BB can be removed, including opening the vacuum sealing at the relevant ports in the cryostat and VV (thus allowing air at room temperature to enter the machine), draining of the fluids from the BB segments, cutting of the cooling pipes, and removal of the shield plugs from the upper port. Given the long time available for the air to circulate in the machine, it is assumed to reach thermal equilibrium with the surfaces at a higher temperature, that is, 300 °C (the temperature of the BB); note that this is a conservative assumption. It must be noted that the divertor should be removed first and not considered in place while removing the BB; however, due to the uncertainty about the RM procedure at the time when the model was built, its surfaces have been included in the model. This is not expected to affect significantly the results.

The suitability of the model employed for the simulation of the natural convection case is discussed in detail in [8], where the physical model as well as the choice of the mesh (especially in the gap region, which is the most critical in terms of temperature and velocity gradients) have been validated in simple cases against available correlation, in order to guarantee the adequacy of the computational model, at least in a simple, but still representative case. Concerning the model employed for the forced convection case, a different set of equations is solved, as the flow is turbulent, as well as a different mesh is employed. In order to guarantee the accuracy of the model, also, in this case, several validation tests on simplified cases (for which empirical correlations are available) have been carried out and they are discussed in Appendix A.

In the case of forced convection, as the forced mass flow rate is much larger than that resulting from natural convection, the contribution of the latter term is neglected; the validity of this assumption has been checked a posteriori by computing the Richardson number Ri (see the following equation):

$$\mathrm{Ri} = \frac{g\beta(T - T_{\mathrm{ref}})L}{v^2} = \frac{\mathrm{Gr}}{\mathrm{Re}^2} \tag{1}$$

where g is the gravity acceleration, $\beta = 1/T_{\mathrm{ref}}$ is the fluid thermal expansion coefficient, $T_{\mathrm{ref}} = 300$ °C is the reference temperature, L is the characteristic length, and v is the fluid velocity. Ri can be interpreted as the ratio between buoyancy forces and inertial forces and can be expressed in terms of the Grashof number Gr and Reynolds number Re. When $\mathrm{Ri} < 0.1$ (which is true in most of the domain in this case; see Section III-B), the buoyancy term can be neglected. This simplification allows solving the Navier–Stokes equations with the segregated approach for pressure–velocity coupling, simplifying the convergence of the numerical model, as opposed to the natural convection case where, due to the tight coupling of the equations via the buoyancy term, the coupled approach must be used [7]. In addition, as the flow field is not driven by the temperature, but only by an external source, it reaches a steady state in few minutes, after which it needs not to be solved anymore. This freezing of the flow field reduces the thermal–hydraulic problem to a pure thermal problem, that is, only the energy conservation equation in solid and fluid needs to be solved, significantly improving the speed of the simulation.

The computational domain, together with the BCs, is reported in Fig. 2; note that, as specified in Fig. 2(a), for the equatorial port two different BCs are used, that is, wall (no-slip, fixed temperature) for the case of natural convection, and fluid inlet with fixed mass flow rate for the case of forced convection (for both cases, the air inlet temperature is 26 °C). Indeed, for the case of natural convection, the equatorial port is assumed to be sealed, according to the same strategy used in [8], whereas, for the case of forced convection, the flow is assumed to be forced via the equatorial port. In the absence of information to evaluate the air mass flow rate, a value of 10 kg/s has been assumed. The first wall (FW), VV, and divertor surfaces are kept at a fixed temperature, equal to the inlet temperature of their respective coolants, as reported in Fig. 2(a). As in the previous analyses,

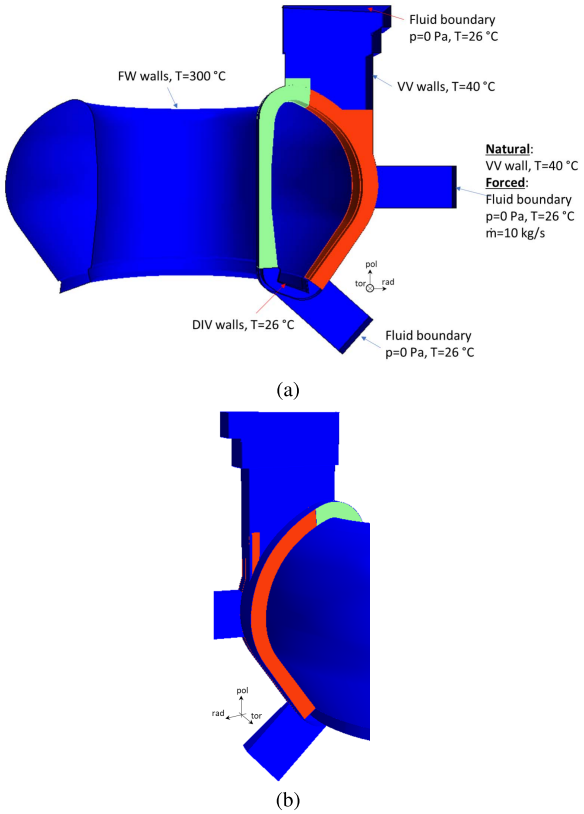

Fig. 2. Computational domain and BCs. (a) View from the symmetry plane. (b) Rearview.

it is assumed that all the BB segments not belonging to the maintained sector are still connected to the PHTS and can thus be kept actively at 300 °C in order to prevent the embrittlement of the EUROFER [10] in the remaining segments; since a PHTS loop is actually feeding more than one sector [11], it is equivalent to assume that isolation valves are available on the hot and cold leg of each sector (at most). The actual applicability of isolation valves is questionable and still under investigation [11], [12], and the choice to implement them or not will require a tradeoff between the clear advantages in the nonoperating phases, such as the maintenance considered in this work (as well as during some accidental transients), and the disadvantages they introduce (e.g., additional pressure drops, the possibility of spurious closure, manufacturability, among others). Consequently, this assumption might need to be revised in the future, and other scenarios are being considered, for example, assuming that all the segments belonging to the same cooling loop are not active anymore. However, this is beyond the scope of this work, whose main aim is to describe the numerical model and the solving strategy adopted, which is flexible and applicable also to other scenarios or designs.

Concerning the initial condition, stagnant (zero velocity) air at 0 Pa (gauge) is assumed to fill the volume. A uniform temperature of 300 °C is assumed, as the air has been let free to enter the domain while draining the segments and cutting the BB coolant pipes, and it is considered to go to equilibrium

TABLE I
FITTING CONSTANTS FOR THE DECAY HEAT FUNCTION

Constant	Value
a	−0.001 165
b	0.052 23
c	−0.8366
d	5.201
f	0.008 689

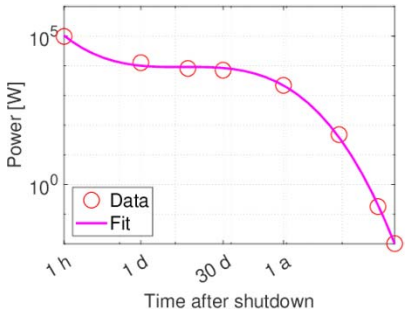

Fig. 3. Decay heat data and comparison with the fitting function.

with the FW surfaces during this time frame (assumed as one month).

As the thermal driver, the decay heat in the steel only is considered, since PbLi has been drained before the transient under consideration. The decay heat is applied to the BB segments under maintenance. The decay heat data has been taken from [13] and fit to a continuous function, which is reported in the following equation:

$$\ln(q''') = a\ln(t+t_0)^4 + b\ln(t+t_0)^3 + \\ +c\ln(t+t_0)^2 + d\ln(t+t_0) + f \quad (2)$$

where q''' is the volumetric power in W/m^3, t is the time in seconds, and t_0 is the start time of the transient since reactor shutdown in seconds (assumed equal to one month as mentioned above). The value of the fitting constants is reported in Table I, whereas a visual comparison of the data and fitting function is shown in Fig. 3.

As for the case of the HCPB, very different space and time scales are found in this problem. To speed up the solution, a strongly nonuniform mesh is employed; for the natural convection scenario, a structured hexahedral mesh is used in the 20 mm gaps between the BB segments and the other components (VV, DIV), featuring three control volumes in the gaps [see the inset in Fig. 4(b)], whereas an unstructured polyhedral mesh is used in the remainder of the fluid domain, as well as in the solid domain. For the forced convection scenario, instead, since the flow is turbulent (see below), a finer mesh has to be used, in particular, in the gaps. These regions have been now meshed with an unstructured polyhedral mesh, coupled with five prism layers; the thickness of the first (near-wall) prism is 20 μm, and the total thickness of the five prism layers is 4 mm. A view of the two computational grids is shown in Fig. 4; they feature about 400 thousand cells (29 million for the forced convection case), and about 90% (96%) of them are located in the region of the maintained sector.

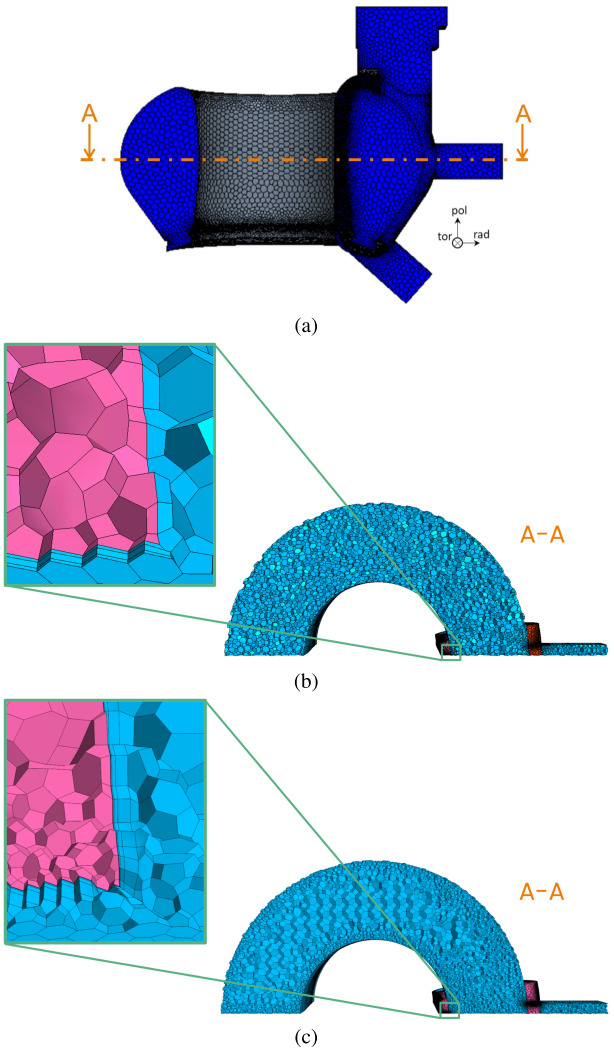

Fig. 4. Computational mesh used in the work. (a) Front view. (b) Cut view (natural convection scenario), with detail of the gap region. (c) Cut view (forced convection scenario), with detail of the gap region.

As far as the time scales are concerned, the convection and conduction time scales (characteristic of the heat transfer in the solid domain), estimated in [8], are about 10^5 s, whereas the advection time scale (characteristic of the fluid) is about 1 s in the natural convection case and about 0.1 s in the forced convection case. Therefore, to accelerate the solution, the solid and fluid problems are partially decoupled: the fluid physics is solved with a time step ten times smaller than the solid physics, and the relevant information at the interface (temperature and heat transfer coefficient) is exchanged every solid time step. In the forced convection simulation, this is done only for the first few minutes of transient, until the flow field reaches a steady state: at this point, as the flow is frozen, the advection timescale is not relevant and the solid and fluid energy conservation equations are solved with the same time step.

The natural convection scenario is assumed to be laminar, as the Rayleigh number Ra, computed according to the following equation:

$$\mathrm{Ra} = \frac{\rho g \beta (T_s - T_\infty)\delta^3}{\mu \alpha} \tag{3}$$

TABLE II
VOLUME COMPOSITION OF THE WCLL BB [14]

Material	COB [m^3]		L/ROB [m^3]		IB [m^3]	
EUROFER97	6.11	(28 %)	5.75	(28 %)	5.17	(32 %)
PbLi	12.9	(59 %)	12.1	(59 %)	8.88	(54 %)
Water	2.64	(12 %)	2.48	(12 %)	2.30	(14 %)
Tungsten	0.0470	(0.22 %)	0.0440	(0.22 %)	0.0490	(0.30 %)

is $\lesssim 3 \times 10^5 \ll 1 \times 10^9$ at any time in the transient, assuming the solid surface temperature $T_s = 300$ °C, and the fluid bulk temperature $T_\infty = 26$ °C; in (3), ρ is the fluid density, $\delta = 20$ mm is the thickness of the gap between the BB segments, μ is the fluid dynamic viscosity, $\alpha = k/(\rho c)$ is the fluid heat diffusivity, k is the fluid thermal conductivity, and c is the fluid specific heat.

Conversely, the flow regime in the forced convection scenario is turbulent, as estimated by the Reynolds number Re (see the following equation):

$$\mathrm{Re} = \frac{\rho v D_H}{\mu} \tag{4}$$

which is $\gtrsim 5 \times 10^3$ at any time during the transient, considering for v the velocity corresponding to the inlet mass flow rate. The hydraulic diameter D_h is computed considering the cross section of the space between two adjacent BB segments, that is, a rectangle 2×100 cm.

Finally, in order to simplify the model, the internals of the BB segments are not modeled in detail, but a uniform, homogeneous material is assumed. The homogenized material properties (density ρ, thermal conductivity k, and specific heat c) are obtained as volume (ρ, k) or mass (c) average values [8], in order to preserve the total solid mass, heat diffusivity, and heat capacity, respectively. As both fluids (water and PbLi) in the segments are assumed to be drained before the maintenance, 97.5% of the volume occupied by water and PbLi is replaced by another gas (assumed in this case to be nitrogen). The volumes of the different materials in the WCLL BB are reported in Table II for a central outboard (COB) segment, a left/right outboard (L/ROB) segment, and an inboard (IB) segment, whereas the values of the thermophysical properties are reported in Table III. Note that for ρ and k, due to their small variation in the temperature range of interest, a constant value is assumed (equal to the value reported in Table III), whereas for c a polynomial fit is adopted, which is reported in the following equation:

$$c_{\mathrm{COB}} = 3.70 \cdot 10^6\ T^3 - 5.72 \cdot 10^3\ T^2 + 3.13\ T - 103 \tag{5a}$$

$$c_{\mathrm{IB}} = 3.81 \cdot 10^6\ T^3 - 5.88 \cdot 10^3\ T^2 + 3.23\ T - 114 \tag{5b}$$

where T is the solid temperature in °C and c is in J/(kg K).

A summary of the validation of the modeling choices and meshing strategy is available in Appendix A; more details are available in [16].

III. RESULTS

A. Natural Convection

Fig. 5 shows the evolution of the maximum temperature in the solid domain, for both IB and OB blanket segments

TABLE III
MATERIAL PROPERTIES @ 300 °C

Material	k [W/(m K)]	c [J/(kg K)]	ρ [kg/m^3]
EUROFER97 [10]	30.0	547	7690
PbLi [14]	13.3	200	9830
Water[a] [15]	0.0440	2010	0.376
Tungsten [14]	125	145	19 300
Nitrogen (ideal gas)	0.0440	1040	0.591
Homogenized (C/L/ROB)	29.7	524	2470
Homogenized (IB)	29.6	516	2470

[a] NB: after coolant drainage, the system is at environment pressure (1 bar); therefore, at 300 °C, water is fully vaporized.

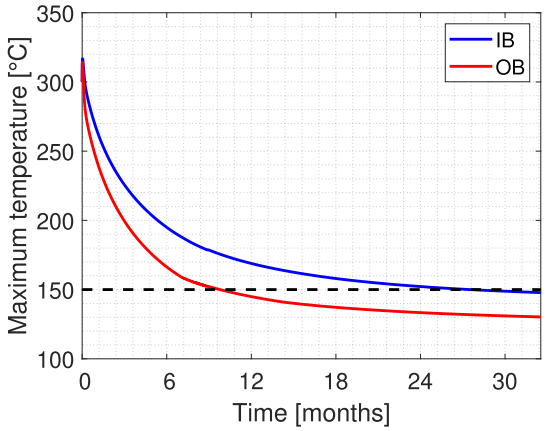

Fig. 5. Evolution of the maximum temperature in the IB and OB segments, in the natural convection case.

in the natural convection case. Qualitatively, the behavior of the system is the same as for the HCPB [8], however, due to the decay heat, which is much larger in the WCLL case, the transient time scale is considerably different, with almost one year required for the cool-down of the OB segment below the 150 °C threshold, and more than two years needed for the IB (it is important to recall that, in the current RH scheme, the OB will be removed first). For the same reason, the initial heat-up phase of the transient (when the natural circulation is not yet enough to counteract the decay heat) brings the maximum value of the temperature to larger values (up to 320 °C).

As for the HCPB, this can be explained considering the evolution of the air temperature in the domain, which is reported in Fig. 6 in terms of maximum and volume-averaged values, together with the volume-averaged value of the solid temperature. Indeed, the average fluid temperature decreases sharply at the beginning of the transient, but the maximum value stays very close to 300 °C, due to the presence of the FW walls being actively kept at this temperature in the nonmaintained sectors (incidentally showing the importance of including them in the model). Since hot air can only flow out from the upper port in the maintained sector, it will also heat up the segments therein. Therefore, in future work, it would be interesting to analyze the natural convection assuming different temperatures of the neighboring BB segments, and the possibility to perform the RM operation in parallel for two or more sectors.

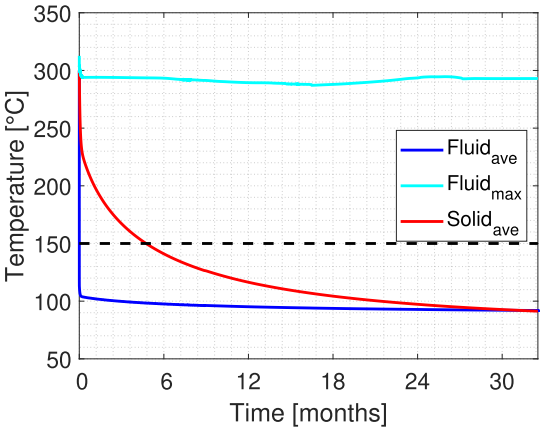

Fig. 6. Evolution of the average fluid and solid temperature in the domain, and of the maximum fluid temperature, in the natural convection case.

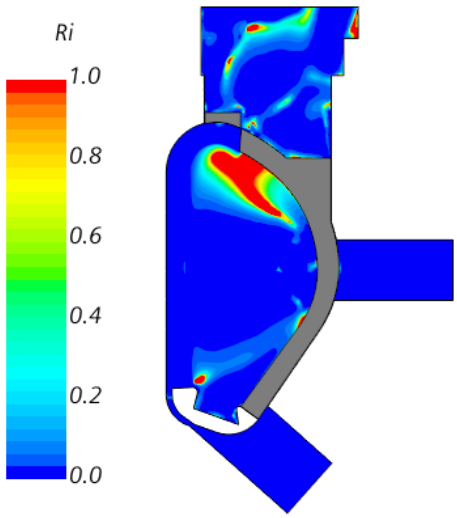

Fig. 7. Map of Ri on the symmetry plane.

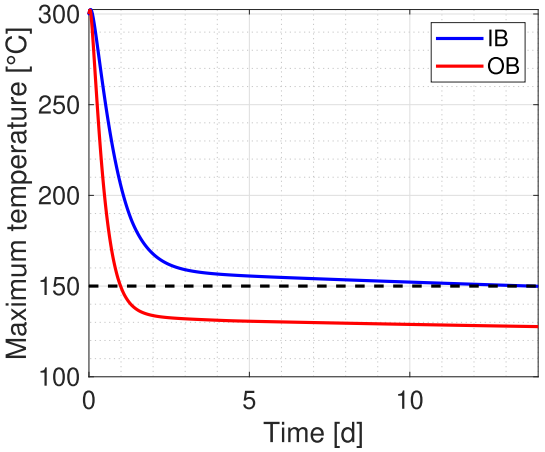

Fig. 8. Evolution of the maximum temperature in the IB and OB segments, in the forced convection case.

In addition, the transient naturally slows down when the solid average temperature approaches the fluid average temperature (see Fig. 6), yielding the exponential-like behavior

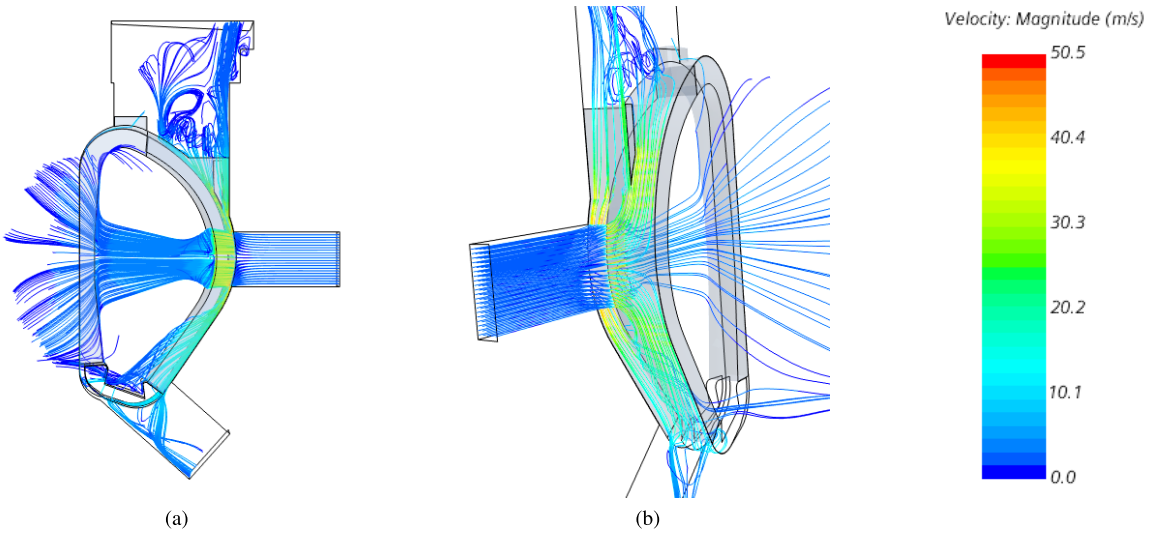

Fig. 9. Steady-state streamlines in the forced convection case. (a) Front view. (b) Rearview.

of the maximum temperature that is visible in Fig. 5. For this reason, it is possible in principle to reduce significantly the cool-down time with a small increase in the operational limit: if, for instance, the RH requirement can be increased up to 160 °C (i.e., 10 °C more), the cool-down time for the OB would pass from ten to seven months, whereas that for the IB would go from 28 to 17 months, that is, around 30% reduction for OB and 40% for IB. In absolute terms, however, this time is still too large, as overall the replacement of a single BB segment may require as long as one year of plant unavailability.

B. Forced Convection

As mentioned in Section II, the assumption of negligible natural circulation is checked by computing the value of Ri, which is <0.1 in most of the domain, as visible in Fig. 7, which reports the distribution of Ri at the beginning of the transient, that is, in the least favorable condition, as the temperature difference at the numerator in (1) has the maximum value at the beginning. Nevertheless, it is advisable to investigate the effects of this assumption, at least in the initial phase of the transient, by comparing it with a simulation including also natural convection.

In the forced convection scenario, the cool-down time for the OB segment is reduced to one day (i.e., more than two orders of magnitude), whereas that for the IB is also reduced to about two weeks (see Fig. 8). In addition to the (obvious) speedup deriving from the larger fluid velocity (and heat transfer coefficient, consequently), this behavior is ascribable to two additional advantages of the forced convection scenario with respect to the natural convection one: first, the flow is forced from the equatorial port, meaning that the fresh air is entering the domain in a location closer to the point of interest for RH (i.e., the upper port); second, the flow driver does not reduce as the transient goes on, being independent on the temperature field. The first is evident looking at Fig. 9, which shows how nearly half of the fresh air is diverted toward the upper port; in addition, the air accelerates through the gap reaching high velocities and, therefore, high heat transfer coefficients (HTCs).

TABLE IV
SURFACE-AVERAGED HEAT TRANSFER COEFFICIENTS

Scenario	OB [W/(m^2 K)]	IB [W/(m^2 K)]
Natural	1.8	1.7
Forced	24	6.0

The different value of HTC between the natural and forced convection cases is also reported in Table IV and Fig. 10, where it is evident how in the forced convection scenario it is about ten times larger, and also how the cooling is beginning closer to the upper port region. Moreover, the HTC in the forced convection case is much less uniform than in the natural convection case, and, in particular, the difference between IB and OB segments is very large in the first, causing the larger (in relative terms) discrepancy in cool-down times between IB and OB in this case. Moreover, this highlights that, even more for the forced convection scenario, lumped models such as those proposed in [8] and [9] are not applicable.

It is important, however, to note that a forced convection cool-down would require the presence of an active cooling system, which would need to be connected to the vacuum vessel before maintenance; such a system would need to be able to withstand significant dose rates and would increase the plant complexity and the down time, making it hard to draw a complete comparison of the two approaches.

IV. CONCLUSION AND PERSPECTIVE

The cool-down transient for a sector of the EU DEMO WCLL BB has been analyzed by means of 3-D transient CFD. Two distinct models have been set up, in order to compare two cooling options, that is, a passive one based on natural convection only, and an active one based on forced convection. Results have shown that the simplest, passive

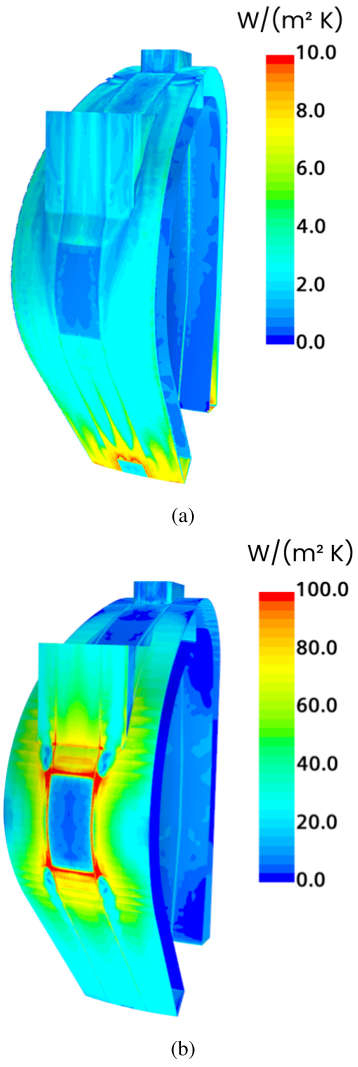

Fig. 10. Heat transfer coefficient on BB surfaces. (a) Natural convection. (b) Forced convection. Note the different scales.

option is insufficient to cool-down the BB segments before maintenance in a reasonable time, requiring several months to reach the threshold of 150 °C required by the RH tools, whereas the active option performs much better, at the price of the increased complexity of the plant. This option allows removing the OB segment already after one day, while the IB segment can be removed after two weeks. The results also highlighted the need for 3-D analyses of the blanket segments as well as of the plasma chamber volume, due to the strong nonuniformity of the cool-down and nonnegligible toroidal flow into the plasma chamber.

In perspective, the model could be applied to investigate the effect of some parameters on the cool-down time, such as the time before the start of the transient (i.e., the time needed to cut the coolant piping), or the draining of the fluids (water and/or PbLi) from the BB segments. In addition, the effect of the disconnection from the PHTS of the adjacent segments, if isolation valves will not be available, will be investigated, as well as the effect of a different temperature of the neighboring BB segments.

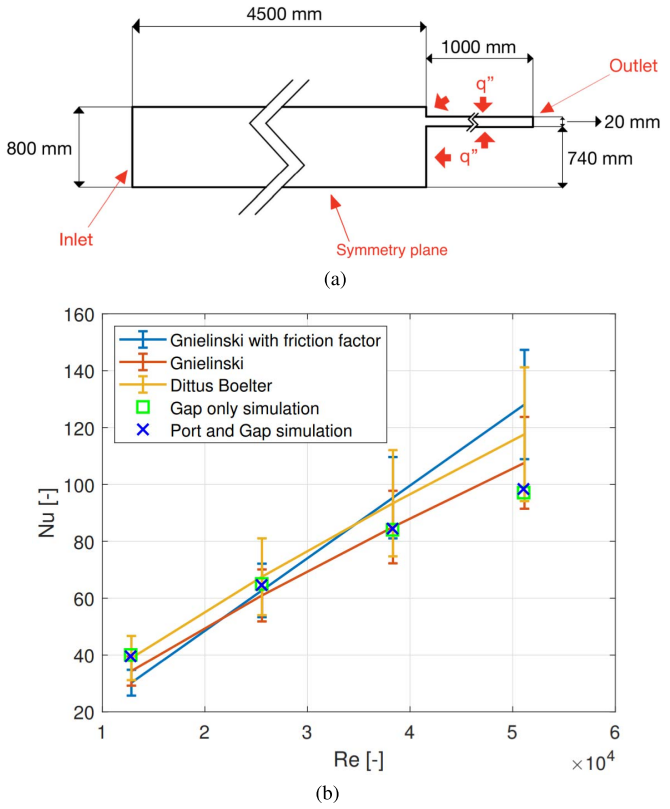

Fig. 11. (a) Sketch of the 2-D domain and BCs used to simulate the port and gap regions. (b) Computed Nusselt values compared with correlations available in the literature.

APPENDIX A

In this appendix, the validation tests performed on simplified cases of the forced convection case are shortly described; for full details on the validation procedure, the reader is referred to [16]. The aim is to focus the attention on simple cases for which empirical correlations are available, but that are representative of the most crucial region of the full 3-D simulation. In this case, the focus is on the gap region, in the portion of the domain where air enters the plasma chamber from the equatorial port.

First, we focused on the heat transfer problem in the gap only. A 2-D rectangular duct, 2-m-long, 2-cm-thick, heated on the two long sides was simulated. The mass flow rate of air was imposed knowing the total mass flow rate entering the equatorial port. The grid independence carried out on the mesh core cell size and on the number of prism layers allowed us to choose the most suitable mesh in the region, without the need of running the entire 3-D transient model. The Nusselt number (Nu) computed in the gap-only simulation was compared to correlations available in the literature, such as the Dittus–Boelter correlation [17] and the Gnielinski correlation (with and without employing the friction factor in the Nu correlation) [18] [see the results gap-only in Fig. 11(b)]. In the entire range of Re scanned, the error, computed according to [19], is always below 1%.

Second, we focused on the hydraulic problem of the sudden contraction from the equatorial port to the gap region. In this case, the gap and port regions were simulated together,

neglecting the effect of the upper and lower walls of the port, thus employing a 2-D model [see Fig. 11(a)]. The interest, in this case, was to assess the accuracy of the model in reproducing the expected localized pressure drop due to the sudden contraction. Available contraction coefficients are available in the literature, for example, in [20]. The coefficient for the sharp-edged entrance region given for circular tubes with symmetric contraction was chosen, which is equal to 0.5, independent of the Re. The computed results were always within 10% with respect to the literature value, keeping in mind that in our case the asymmetry of the gap is considered and the contraction is that for a rectangular channel rather than a circular tube. Nevertheless, the agreement is satisfactory and this ensures that the flow field computation from the port to the gap region is well reproduced. This assessment was preparatory for the next step.

The third and last step was focused on assessing the heat transfer in this case of port and gap together and, in particular, in the gap region, where the heat coming from the BB segments is present in the 3-D model. The comparison of the Nu computed in the model featuring the port and the gap is shown in Fig. 11(b). Also, in this case, the error between the correlation and the computed results is within 1% over the entire range of Re explored.

These tests allowed assessing the accuracy of the equations (in particular, the turbulence model) and the mesh employed in the model, thus ensuring that, at least in the most critical region in terms of temperature and velocity gradients, the 3-D model can rely on robust building blocks.

ACKNOWLEDGMENT

Computational resources were provided by HPC@POLITO, a project of Academic Computing within the Department of Control and Computer Engineering at the Politecnico di Torino (http://www.hpc.polito.it), Turin, Italy.

REFERENCES

[1] A. J. H. Donné et al., *European Reasearch Roadmap to the Realisation of Fusion Energy*. Garching, Germany: EUROfusion Consortium, Sep. 2018.
[2] F. Cismondi et al., "Progress in EU breeding blanket design and integration," *Fusion Eng. Des.*, vol. 136, pp. 782–792, Nov. 2018.
[3] G. A. Spagnuolo, G. Bongiovi, F. Franza, and I. A. Maione, "Systems engineering approach in support to the breeding blanket design," *Fusion Eng. Des.*, vol. 146, pp. 31–35, Sep. 2019.
[4] J. Keep, S. Wood, N. Gupta, M. Coleman, and A. Loving, "Remote handling of DEMO breeder blanket segments: Blanket transporter conceptual studies," *Fusion Eng. Design*, vol. 124, pp. 420–425, Nov. 2017.
[5] G. A. Spagnuolo et al., "Integrated design of breeding blanket and ancillary systems related to the use of helium or water as a coolant and impact on the overall plant design," *Fusion Eng. Des.*, vol. 173, Dec. 2021, Art. no. 112933.
[6] P. Arena et al., "The DEMO water-cooled lead-lithium breeding blanket: Design status at the end of the pre-conceptual design phase," *Appl. Sci.*, vol. 11, no. 24, p. 11592, 2021.
[7] *Star-CCM+ v2019.3 User's Manual*, Siemens, Munich, Germany, 2019.
[8] A. Zappatore, A. Froio, G. A. Spagnuolo, and R. Zanino, "CFD analysis of natural convection cooling of the in-vessel components during a shutdown of the EU DEMO fusion reactor," *Fusion Eng. Des.*, vol. 165, Apr. 2021, Art. no. 112252.
[9] M. Draksler, C. Bachmann, and B. Končar, "Assessment of residual heat removal from activated breeding blanket segment during remote handling in DEMO," *Fusion Eng. Des.*, vol. 173, Dec. 2021, Art. no. 112891.
[10] F. Gillemot, E. Gaganidze, and I. Szenthe, *Material Property Handbook Pilot Project on EUROFER97 (MTA EK, KIT)*, document EFDA_D_2MRP77, Feb. 2016.
[11] L. Barucca et al., "Maturation of critical technologies for the DEMO balance of plant systems," *Fusion Eng. Des.*, vol. 179, Jun. 2022, Art. no. 113096.
[12] A. Froio, L. Barucca, S. Ciattaglia, F. Cismondi, L. Savoldi, and R. Zanino, "Analysis of the effects of primary heat transfer system isolation valves in case of in-vessel loss-of-coolant accidents in the EU DEMO," *Fusion Eng. Des.*, vol. 159, Oct. 2020, Art. no. 111926.
[13] T. Berry and T. Eade, *Calculation of Decay Heat in PbLi for Entire WCLL Reactor*, document EFDA_D_2NQL5P v1.0, Mar. 2020.
[14] A. Del Nevo and P. Arena, *WCLL Design Description Document (DDD)*, document EFDA_D_2NGB4U v1.2, Apr. 2021.
[15] W. Wagner et al., "The IAPWS industrial formulation 1997 for the thermodynamic properties of water and steam," *J. Eng. Turbines Power*, vol. 122, no. 1, pp. 150–184, Jan. 2000.
[16] N. Garelli, "Analysis of different options for the cooling of in-vessel components in DEMO fusion reactor," M.S. thesis, Dipartimento Energia, Politecnico di Torino, Turin, Italy, Mar. 2021.
[17] F. Incropera and D. Dewitt, *Fundamentals of Heat and Mass Transfer*, 7th ed. Hoboken, NJ, USA: Wiley, 2011.
[18] N. Todreas and M. Kazimi, *Nuclear Systems*, 2nd ed. Boca Raton, FL, USA: CRC Press, 2011.
[19] P. J. Roache, "Perspective: A method for uniform reporting of grid refinement studies," *J. Fluids Eng. Trans. ASME*, vol. 116, no. 3, pp. 405–413, 1994.
[20] B. Munson, A. Rothmayer, T. Okiishi, and W. Huebsch, *Fundamentals of Fluid Mechanics*, 7th ed. Hoboken, NJ, USA: Wiley, 2013.

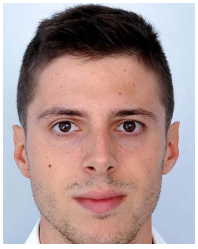

Nicolò Garelli received the B.Sc. degree and the M.Sc. degree in energy and nuclear engineering from the Politecnico di Torino, Turin, Italy, in 2018 and 2021, respectively.

From 2019 to 2020, he spent six months at SCK-CEN: Belgium Nuclear Research Centre, Mol, Belgium, in the framework of a European Mobility Program. During this period, he attended some courses of the BNEN master-after-master program in nuclear engineering, and he took part in a number of activities in the research center's laboratories. In early 2021, while finishing his master thesis, he started his professional career in the technical office of MM construction, a company that deals with the design and construction of industrial plants. Since late 2021, he has been working full-time as a Thermal-Hydraulic Analyst, dealing mainly with CFD analyses, at newcleo, Turin, Italy, a young and innovative nuclear energy company.

Antonio Froio received the B.Sc. degree in mechanical engineering from the Università della Calabria, Rende (CS), Italy, in 2012, the M.Sc. degree in energy and nuclear engineering from the Politecnico di Torino, Turin, Italy, in 2014, the M.Sc. degree in nuclear engineering from the Politecnico di Milano, Milan, Italy, under a double degree program, in 2015, the Alta Scuola Politecnica Diploma degree from the Politecnico di Torino and the Politecnico di Milano in 2015, and the Ph.D. degree in energetics from the Politecnico di Torino in 2018.

From 2018 to 2021, he was a Research Fellow with the Department of Energy, Politecnico di Torino, where he has been an Assistant Professor since 2022. He has authored or coauthored more than 30 articles in international journals concerning the development and application of system-level models for tokamak fusion reactors, the CFD analysis of different fusion components, and the multiphysics modeling of the breeding blanket. He is involved in the design of the EU DEMO in-vessel components and related auxiliary systems. He is a co-inventor of two patents.

Dr. Froio is a member of the American Nuclear Society and the Associazione Italiana Nucleare. He was awarded the EUROfusion Engineering Grant in 2018.

Gandolfo Alessandro Spagnuolo received the master's degree in energy and nuclear engineering from the University of Palermo, Palermo, Italy, in 2014, and the Ph.D. degree in mechanical engineering and energy and information technologies jointly by the Karlsruhe Institute of Technology (KIT), Karlsruhe, Germany, and the University of Palermo, in 2020.

From 2012 to 2013, he was a Fellow Researcher with the University of Palermo working on the thermal-hydraulics of the divertor, test blanket module, and shielding blankets of ITER reactors. In 2013, he was an Intern at ITER, Cadarache, France, working on the definition of the procedure for the study of the whipping effects of high-energy piping. From 2014 to 2015, he worked as a Thermal-Hydraulic and Thermo-Mechanic Analyst as well as a System Engineer at Kraftanlagen Heidelberg GmbH. From 2015 to 2018, he was awarded the EUROfusion Engineering Grant for support to the design of the DEMO breeding blanket concepts. Since 2015, he has been a Researcher at KIT, where he concluded the EEG and the Ph.D. while working for the Management and Support Design Integration Team (MDIT) on project control, system engineering, and requirements definition and management. Since 2020, he has been seconded at EUROfusion, where he covered several roles, such as a Breeding Blanket Design Integration Engineer and a Senior Coordinator for TBM Research and Development activities as well as the Area Manager for the integration of the in-vessel components. He has authored or coauthored more than 30 scientific articles in international peer-reviewed journals.

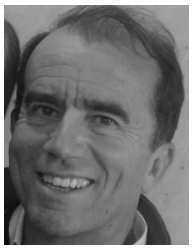

Roberto Zanino (Senior Member, IEEE) received the M.Sc. degree in nuclear engineering and the Ph.D. degree in energetics from the Politecnico di Torino (PoliTo), Turin, Italy, in 1984 and 1989, respectively.

He has been a Professor of nuclear engineering with the Department of Energy, PoliTo, since 2000. He has authored or coauthored over 200 articles that appeared in international journals devoted to the computational modeling in the fields of relevance for nuclear fusion (superconducting magnets and cryogenics, plasma–wall interactions, and high heat flux components), nuclear fission (Gen-IV lead-cooled fast reactors), and concentrated solar power (central tower system receivers).

Prof. Zanino is a member of the American Nuclear Society and regularly serves as a Referee of the IEEE TRANSACTIONS ON APPLIED SUPERCONDUCTIVITY.

Andrea Zappatore received the M.Sc. degree in energy and nuclear engineering and the Ph.D. degree in energetics from the Politecnico di Torino (PoliTo), Turin, Italy, in 2016 and 2021, respectively.

He is currently a Research Assistant at PoliTo. He has coauthored over 25 articles published in international journals focused on computational modeling in nuclear fusion systems and components. His research interests include the development, verification, validation, and application of new modeling tools for both low and high-temperature superconducting magnets and the computational fluid dynamics modeling of high heat flux components as well as of accidental scenarios.

Dr. Zappatore was awarded in 2021 with an EUROfusion Researcher Grant for the development and validation of quench and AC loss models for high-temperature superconducting cable-in-conduit conductors for the EU-DEMO Central Solenoid.

Open Access funding provided by 'Politecnico di Torino' within the CRUI CARE Agreement